Application of polymerized multiporous nanofiber of SnO2 for designing a bienzyme glucose biosensor based on HRP/GOx

Samiul Alim, A.K.M. Kafi, Jose Rajan, Mashitah M. Yusoff

PII: S0141-8130(18)35479-5
DOI: https://doi.org/10.1016/j.ijbiomac.2018.11.171
Reference: BIOMAC 11048

To appear in: *International Journal of Biological Macromolecules*

Received date: 13 October 2018
Revised date: 14 November 2018
Accepted date: 17 November 2018

Please cite this article as: Samiul Alim, A.K.M. Kafi, Jose Rajan, Mashitah M. Yusoff , Application of polymerized multiporous nanofiber of SnO2 for designing a bienzyme glucose biosensor based on HRP/GOx. Biomac (2018), https://doi.org/10.1016/j.ijbiomac.2018.11.171

Application of polymerized multiporous nanofiber of SnO_2 for designing a bienzyme glucose biosensor based on HRP/GOx

Samiul Alim, A.K.M. Kafi, Jose Rajan, Mashitah M. Yusoff*

Faculty of Industrial Sciences & Technology, Universiti Malaysia Pahang, Kuantan 26300, Malaysia

*Correspondence should be addressed to A.K.M. Kafi.

Email: kafiakm@ump.edu.my

Tel.: +609 549 2392

Fax: +609 549 2766

Abstract

This work reports on a novel glucose biosensor based on co-immobilization of glucose oxidase (GOx) and horseradish peroxidase with polymerized multiporous nanofiber (MPNFs) of SnO_2 onto glassy carbon electrode with chitosan. Multiporous nanofibers of SnO_2 were synthesized by electrospinning method from the tin precursor which possesses high surface area good electrical conductivity, and the nanofibers were polymerized with polyaniline (PANI). GOx and HRP were then co-immobilized with the nanofibers on the surface of the glassy carbon electrode by using chitosan. The polymerized nanofibers play a significant role in facilitating the direct electron transfer between the electroactive center of the immobilized enzyme and the electrode surface. The morphology of the nanofiber and polymerized nanofiber has been evaluated by field emission scanning electron microscopy (FESEM). Cyclic Voltammetry and amperometry were employed to study and optimize the performance of the fabricated biosensor. The PANI/SnO_2-NF/GOx-HRP/Ch/GC biosensor displayed a linear amperometric response towards the glucose concentration range from 5 to 100 μM with a detection limit of 1.8 μM (S/N = 3). Also, the anti-interference study and real sample analysis was investigated. Furthermore, the biosensor reported in this work exhibited excellent stability, reproducibility, and repeatability.

1. Introduction

Distinctive features of nano-sized materials like higher surface area enhanced electrical conductivity, and excellent chemical and thermal stability have made them suitable for use in the health and environment. It is reported that these nanomaterials play an essential role in obtaining direct electron transfer of redox proteins or enzymes from the active site of them to the electrode surface [1, 2]. Nevertheless, a lot of researches have been conducted over the last few decades to obtain more advanced nanomaterials with upgraded features, and their application is perceived in the development of electrochemical biosensors [3-5]. Among this abundance of nano-sized materials, SnO_2 nanomaterials have received much attention and being used widely as nanotubes, nanoparticles, nanowires, and nanorods [6, 7]. With features like high surface area, nontoxicity, excellent biocompatibility, catalytic activity, and chemical stability [8], nanostructured SnO_2 became convenient for diverse applications such as solar cells, electrochemistry, and biosensor [9-11]. We reported a new one-dimensional nano-morphology of SnO_2 recently in our previous work [11] with the higher surface area and higher electron mobility characteristics, named as multiporous nanofibers (MPNFs). It was synthesized through electrospinning method by controlling the tin precursor concentration [12], and this potential nanofiber showed excellent performance in biosensing [11, 13].

Moreover, the inclusion of polymer such as polyaniline (PANI) with this nanofiber can be an incentive for the advancement of biosensor due to its propensity of intensifying the electrical conductivity and abolition of electrode fouling [14] accompanied by some other characteristics like mechanical flexibility, thermal and chemical stability [15, 16]. PANI sustains redox cycling and can help in obtaining direct electron transfer from the enzyme active site to the electrode surface when used in enzymatic biosensor [17]. The combination of PANI and MPNFs of SnO_2

have been proved as an excellent platform for electrochemical sensing applications as both of these two materials showed excellence in different work during the construction of electrochemical sensors and biosensors [11, 18, 19].

Selective and sensitive detection of glucose with faster response time is of great importance for the last decades due to its necessity in industrial and clinical aspects [2, 20]. Different methods for glucose analysis have been reported such as flow injection [21], fluorescence [22], electrochemistry [23], etc. But the amperometric enzyme-based biosensor technology gained much admiration due to their simplicity, faster response and higher sensitivity with excellent selectivity. Mostly, the glucose detection through enzyme-based biosensors is accomplished by the electrochemical detection of hydrogen peroxide, engendered in the enzymatic reaction of the glucose oxidase (GOD). However, a considerable drawback of this procedure is represented by high over-potential required for hydrogen peroxide oxidation (exceeding 0.6 V versus Ag/AgCl). This causes the loss of selectivity due to the oxidation of some electroactive substances present in real samples, such as ascorbic acid, uric acid, and acetaminophen under this potential [24]. Therefore, different strategies have been exploited to eliminate the interference and thus to boost the selectivity of enzyme-based biosensors. The effective tactic to overcome this interference issue involved the adoption of a redox mediator such as Prussian blue [25] or peroxidase [26] to reduce the positive working potential which could also improve the electron transfer between enzyme and electrode [27]. The most common redox mediator in this issue is horseradish peroxide (HRP) for the reduction of H_2O_2 as electrons relay due to the intrinsic selectivity and intensification of the enzymatic reaction. In such a system, hydrogen peroxide produced from the glucose oxidation step by oxygen with the aid of GOD is subsequently catalytically reduced by HRP. The oxidized state of horseradish peroxidase ($HRP_{(ox)}$) is then electrically connected to the

electrode surface either by a free diffusing mediator or directly communicating electrons with the electrode at low applied potentials.

This work aims to take advantage of the direct electron transfer capability of HRP to the electrode surface with an endeavor to design novel amperometric enzymatic biosensor based on co-immobilization of GOD and HRP with polymerized multiporous nanofiber of SnO_2. Multiporous nanofibers of SnO_2 were synthesized by electrospinning method from the tin precursor. Followed by the synthesis of SnO_2-NF, polyaniline (PANI) has been polymerized on SnO_2-NF to develop PANI/SnO_2-NF composite. Experimental results divulge that the electrochemical glucose biosensor showed fast response with high sensitivity, low detection limit & higher stability and selectivity. Amperometric response and real sample analysis indicate the linearity of the fabricated biosensor and excellent electrocatalytic activity towards the detection glucose in real sample, which opens up a new avenue for developing excellent electrochemical biosensors in recent future.

2. Experimental

2.1. Reagents and materials

Tin chloride pentahydrate ($SnCl_4.5H_2O$), polyvinylpyrrolidone (PVP) and dimethylformamide (DMF) were obtained from Sigma. Glucose oxidase (GOD), Horseradish Peroxidase (HRP), D-glucose, chitosan and a stock solution of H_2O_2 (30 wt %) were also bought from Sigma and was used as received and preserved at 4 ^oC. Aniline monomer (99.5%) and ammonium persulfate for polymerization (APS, 98%) were purchased from E. Merck (Germany). The Nanopure® water system was used in this work to purify the pure water (18 MΩ. cm) for preparing all the solutions. All other reagents were of analytical grade, and 0.01 M Phosphate buffer of pH 7.0

was freshly made each time before using. The pH of the phosphate buffer was adjusted by using 1.0 M sodium hydroxide (NaOH).

2.2. Preparation of the SnO_2 nanofiber

Multiporous SnO_2 nanofiber was synthesized according to the protocol discussed in our previous work [11], whereas, the starting reagents were tin chloride pentahydrate ($SnCl_4.5H_2O$), polyvinylpyrrolidone (PVP), dimethylformamide (DMF) and ethanol. Briefly, 3 g of PVP was dissolved in an equal volume ratio (1 : 1) of ethanol and DMF, and different concentrations of the tin precursor were dissolved to this solution at room temperature until the solution becomes transparent. The concentrations of tin precursor solution used in MPNFs synthesis were 5.5 mM, 7 mM, 8.5 mM, 10 mM, 11.5 mM and were labeled as C_0, C_1, C_2, C_3 and C_4, respectively. The viscosity of the solution for electrospinning was measured with a rheometer (LVDV III Ultra, Brook□eld Co., USA) and the solutions were then transferred to a plastic syringe with steel needles. The following parameters was utilized in the procedure: (i) applied voltage, 25 kV, (ii) the injection rate, 0.6 mL h^{-1}, (iii) the distance between the collector and the tip of the needle, 20 cm, (iv) humidity, 40–45%, and (v) 1200 rpm speed of the rotating collector. Solid nanofibers were then collected from the collector and annealed at 600 °C temperature for 3 hour at heating rate 0.5 °C per minute.

2.3. Synthesis of polyaniline (PANI) and PANI-SnO_2-NFs

Followed by the fabrication of SnO_2-NFs, polyaniline (PANI) has been polymerized on SnO_2 using chemical oxidation polymerization method to construct PANI-SnO_2-NF composite [28, 29]. Firstly, Aniline (0.1 M) and ammonium persulphate (0.1 M) were dissolved separately in 0.1 M HCl solution for the synthesis of polyaniline and stirred for 1 h. Then 5 mL of HCL

(0.1 M) and 5 mL of 0.1 M aniline monomer were mixed in 1:1 ratio. 5% solution of oxidant APS prepared in 0.1 M HCl was added dropwise to the above mixture until well-dispersed solution by keeping the temperature between 0–5 °C under continuous stirring. A reasonable degree of polymerization (a greenish black precipitate) was achieved after 3 h. The precipitate yielded in the reaction was separated by filtration, repeatedly washed with distilled water until the pH reached at 7.0 and dried under vacuum for 24 h.

SnO_2 nanofibers were then suspended separately in 0.1 M HCl (13 mL) solution and sonicated for 1 h to minimize accumulation of SnO_2 nanofibers. 10 mL aniline (in 0.1 M HCl) solution and 10 mL SnO_2 nanofibers suspension were mixed and further sonicated for 30 min. 10 mL APS solution was then slowly added dropwise to well-scattered suspension mixture with vigorous stirring at 0–5 °C. The mixture color then turns to greenish after the addition of APS and stirrer is continued to about 5 h. The mixture was then kept overnight to settle the precipitate. A good degree of composite polymerization was perceived after that. The precipitate was washed on the next day with distilled water for several times until pH 7.0, dried in the vacuum oven at 60 °C for 3 h before it was pounded to powder.

2.4. Fabrication of the Biosensor

A stock solution of PANI/SnO_2 NF (1 mg/100 µl) was prepared first followed by the stock solution of 2 mg/ml of HRP and 2 mg/ml of GOx in phosphate buffer (pH 7.0). A glassy carbon electrode (3 mm of diameter) was polished with alumina powder (0.05 µM), rinsed thoroughly with deionized water and acetone subsequently, and then dried at room temperature. Finally, 5 µL of PANI/SnO_2 NF the stock solution and 5 µL of horseradish peroxidase and glucose oxidase from the stock solution were co-immobilized onto the glassy carbon electrode together

with 2 μL of 2 mg/ml of chitosan (Ch). The electrodes used for comparison were fabricated in the same way and was denoted as PANI/SnO_2-NF/Ch/GC, PANI/SnO_2NF/HRP/Ch/GC and PANI/SnO_2-NF/GOx-HRP/Ch/GC respectively. All the electrodes were stored at 4 °C in 0.1 M phosphate buffer at pH 7.0 when not in use.

2.5. Morphological and Electrochemical characterization

Morphological characterization of synthesized nanofiber and polymerized nanofiber was evaluated by field emission scanning electron microscopy (JEOL-USA) at an acceleration voltage of 13kV. The electrochemical measurements were carried out by using Potentiostat PARSTAT 2273 on a CHI (630B) workstation. A three-electrode system was employed, whereas, a modified electrode as the working electrode, a platinum wire as a counter electrode and an Ag/AgCl was used as reference electrode. Cyclic voltammetric (CV) measurements were carried out in 0.1 M phosphate buffer by scanning the electrode potential in the range between 0.1 and -0.6V versus Ag/AgCl. Amperometric responses were measured in 0.1 M phosphate buffer stirred by a magnetic stirrer.

3. Results and Discussions

3.1. Surface characterization of multiporous SnO_2 nanofiber

FESEM was conducted to characterize the morphologies of the MPNFs of SnO_2, PANI/SnO_2-NFs and HRP-GOD/PANI/SnO_2-NFs. The FESEM image (Fig. 1A) represents the morphology of multiporous SnO_2 nanofiber and PANI/SnO_2-NFs. The obtained multiporous SnO_2 nanofiber showed a fibrous structure in all areas with some fiber-fiber interconnections and according to previous work, the MPNFs were constructed with grains size of 5–15 nm and the MPNFs were smaller than the grain size of the PNFs (15–25 nm) [12]. The crystal-like structure is observed in

MPNFs due to the lower grain size. And relatively higher polycrystallinity of MPNFs is also a reason for that structure. The smaller grains and many channels in MPNFs are therefore the sources of its high surface area which allows for a high density proteins/enzyme loading during the development of any biosensor. The elemental analysis of synthesized SnO_2 nanofiber was further done by using energy dispersive x-ray spectroscopy (EDX). As shown in Fig. 1B, emission peaks of Sn and O observed in the EDX spectrum presents the presence of tin and oxygen elements, confirming that the formed MPNFs of SnO_2.

Fig. 2A shows the FESEM image of a polymerized nanofiber of SnO_2. A rough surface of the net-like structure is clearly observed in the image of PANI/SnO_2-NFs which confirms the polymerization of SnO_2 nanofiber with Polyaniline. Moreover, a network line structure is observed in HRP-GOD/ PANI/SnO_2-MPNFs (Fig. 2B) with the aggregation of the immobilized enzyme molecules regularly distributed. When HRP-GOD enzyme was immobilized in the PANI/SnO_2-MPNFs film, the surface of the PANI/SnO_2-MPNFs were not clearly seen suggesting the enzymes wrapped them. The distinguished characters of the FESEM images indicate the presence of an enzyme on the HRP-GOD/PANI/SnO_2-NFs surface.

3.2. Electrochemical behavior of the PANI/SnO_2-NF/HRP/Ch/GC electrode

Fig. 3A illustrates the cyclic voltammograms (CVs) of the (i) bare, (ii) HRP/Ch/GC and (iii) PANI/SnO_2-NF/HRP/Ch/GC electrodes recorded in a 0.1M phosphate buffer (pH 7.0) at a scan rate of 60 mVs^{-1}. As expected, neither oxidation nor reduction peak appeared in the CV of the bare electrode. But a small reduction peak appears in the CV of the HRP/Ch/GCE electrode which is attributed to the reduction of the immobilized HRP at the underlying electrodes. However, well-defined oxidation and reduction peak appear in the CV of the PANI/SnO_2-

NF/HRP/Ch/GC electrode, whereas, the anodic and cathodic peak potentials are located at -0.22 V and -0.38 V respectively. The formal potential $E_n \mid E_n = (E_{pa} + E_{pc})/2$ was calculated to be -0.3 V.

The effect of the scan rates was investigated on the response of PANI/SnO_2-NF/HRP/Ch/GC electrode. Fig. 3B shows the cyclic voltammograms response of resulting PANI/SnO_2-NF/HRP/Ch/GC electrode at a scan rate of 60, 80, 100, and 120 mVs^{-1} (from inside to outside) recorded in 0.1 M phosphate buffer (pH 7.0). The peak-to-peak difference enhances evenly with the enhancement of scan rates. The results suggest that all the electroactive redox enzymes at the PANI/SnO_2-NF/HRP/Ch/GC electrode had been reduced on the forward cathodic scan [30]. These results also imply that the introduction of PANI/SnO_2-NF augments the electrical activity of HRP present in the electrode. Moreover, the polymerized MPNFs of SnO_2 functioned as microelectrodes to connect the active sites of HRP with the underlying electrode by condensing the distance between the redox active site of HRP and the surface of electrode [31].

3.3. The electrochemical response of the PANI/SnO_2-NF/HRP/Ch/GC to H_2O_2

To find out the detecting potential of glucose, the response of the PANI/SnO_2-NF/HRP/Ch/GC to H_2O_2 was investigated. Cyclic voltammograms of the PANI/SnO_2-NF/HRP/Ch/GC electrode recorded in the absence and presence of 10 μM H_2O_2 in 0.1M Phosphate buffer at pH 7.0 at a scan rate of 60 mVs^{-1} is shown in Fig. 4. According to the result, the PANI/SnO_2-NF/HRP/Ch/GC electrode gives its diffusional redox wave in the absent of H_2O_2 in electrolyte (straight line), whereas, with the introduction of hydrogen peroxide to the solution, a sharp enhancement of cathodic current (dashed line) appears with a simultaneous decline in the corresponding anodic peak. This change specifies that the enhanced reduction current in the

presence of H_2O_2 is due to the presence of heme redox active center of immobilized HRP on PANI/SnO_2-NF/Ch/GCE electrode. The results demonstrate that the immobilized HRP possessed excellent electrocatalytic activity towards H_2O_2 reduction. [32]. The electrocatalytic reduction mechanism of H_2O_2 by HRP can be described as follows [33].

$$\text{HRP } (Fe^{3+}) + H_2O_2 \rightarrow \text{Compound I } (Fe^{4+}= O) + H_2O \quad (1)$$

$$\text{Compound I } (Fe^{4+}=O) + e^- + H^+ \rightarrow \text{Compound II} \quad (2)$$

$$\text{Compound II} + e^- + H^+ \rightarrow \text{HRP } (Fe^{3+}) + H_2O \quad (3)$$

3.4. The response of the PANI/SnO_2-NF/HRP-GOx/Ch/GC electrode to Glucose

Fig. 5 shows the Cyclic voltammograms response of PANI/SnO_2-NF/HRP/Ch/GC electrode (dashed line) and PANI/SnO_2-NF/HRP-GOx/Ch/GC electrode (straight line) at scan rate of 80 mVs^{-1} recorded in 0.1M phosphate buffer (pH 7.0). We can see that both the oxidation and anodic current is decreased which occurs due to the blockage of some of the redox reaction sites of immobilized GOD enzyme [34], which suggests the successful immobilization of GOD onto PANI/SnO_2-NF/HRP/Ch/GC electrode. In Fig. 6, the cyclic voltammogram graph shows the response of PANI/SnO_2-NF/HRP-GOx/Ch/GC electrode in the absence (straight line) and the presence of 10 μM glucose (dashed line) in 0.1 M phosphate buffer (pH 7.0) at a scan rate of 80 mV/s. The result shows the enhancement of reduction current, whereas, the oxidation current is decreased. It is occurred due to the oxidation of glucose by the catalytic activity of GOD enzyme immobilized on the electrode. Glucose is catalytically oxidized into gluconolactone and hydrogen peroxide in the presence of dissolved oxygen and GOx enzyme. The resulting H_2O_2

then reacts with the co-immobilized HRP to be reduced. The resulting reaction is as followed [1, 35].

$$\text{Glucose} + \text{GOD(FAD)} \rightarrow \text{gluconolactone} + \text{GOD}(FADH_2) \quad (4)$$

$$\text{GOD}(FADH_2) + O_2 \rightarrow \text{GOD(FAD)} + H_2O_2 \quad (5)$$

$$\text{HRP (red)} + H_2O_2 \rightarrow \text{HRP (ox)} + H_2O \quad (6)$$

3.5. Amperometric Response & Optimization of Experimental Parameters

The influence of the applied electrode potential and pH of the phosphate buffer on the amperometric response of the PANI/SnO_2-NF/HRP-GOx/Ch/GC electrode to glucose was evaluated. The results reveal the optimized applied potential of -0.3 V and pH = 7.0 for glucose sensing. Fig. 7A shows the steady-state amperometric response of the PANI/SnO_2-NF/HRP-GOx/Ch/GC electrode recorded by successively adding glucose into the phosphate buffer under the optimized applied potential and pH. About 95% of the steady-state current was achieved for the PANI/SnO_2-NF/HRP-GOx/Ch/GC electrode at less than 10s. The corresponding calibration curves for the PANI/SnO_2-NF/HRP-GOx/Ch/GC electrodes are displayed in Fig. 7B. A linear relationship of the current was observed to the concentration of glucose between 5 and 100 μM with a correlation coefficient of 0.996. The detection limit (LOD) is calculated to be 1.8 μM glucose (based on S/N = 3).

3.6. Anti-interference Activity of the Glucose Biosensor Biosensor

One of the main challenges in glucose analysis by electrochemical biosensors is the elimination of interfering signals occurred by the electroactive species like uric acid (UA), ascorbic acid

(AA), Dopamine (DA) that co-exist in real samples with glucose and can interfere the activity of glucose biosensor due to the overlapping of the peak which is proportional to the concentration of the analyte [20]. The amperometric response of the biosensor with successive additions of these interfering substances and glucose in 0.1 M phosphate buffer (pH = 7.0) was determined under the applied electrode potential -0.3V to evaluate the selectivity of this fabricated electrode. The biosensor exhibited very strong response to the successive injections of 10μM glucose and very negligible response to 0.1 mM AA and 0.2 mM UA (Fig. 8). The result denotes a very high anti-interferent activity of that fabricated biosensor.

3.7. Real Sample Analysis

Glucose detection in blood and urine is indispensable for the diagnosis of diabetes. Also, some glucose is found in urine during pregnancy, which encouraged our work to use urine for evaluating the efficiency of the fabricated biosensor in detecting glucose in the real sample. The real sample analysis of the fabricated biosensor was carried out through the amperometric response of the fabricated biosensor towards real sample (urine) and glucose in phosphate buffer (pH 7.0) solution. Primarily, we used the urine sample with a known concentration of glucose and compared the amperometric response with the amperometric response found by using fresh glucose. The current increased with each spike of a urine sample (with known concentration) by avoiding the interferences. From the current response vs. concentration curve, it was found that about 96% of the current response obtained from the addition of only glucose was achieved. That performance of the fabricated biosensor signifies the potentiality of the fabricated biosensor in detecting glucose in the real sample.

3.8. Stability and Repeatability of the Glucose Biosensor

The most crucial feature of any biosensor is the stability and repeatability, which is endorsed on several strands. The long-term stability of this fabricated biosensor was estimated by storing the electrode in phosphate buffer (pH 7.0) at 4^0 C for 60 days, and the electrode triumphed 94% of its initial response to glucose. The repeatability of the biosensor for current response was also studied, and the relative standard deviation (R.S.D.) was 3.5% for 10 successive assays using the same electrode. Table 1 summarized comparison of performances of this biosensor with other recent glucose biosensors fabricated with different nanomaterial combination. It is clearly seen that the modified biosensor based on the PANI/SnO_2-NF/HRP-GOx/Ch/GC electrode shows better analytical performance regarding LOD and stability.

4. Conclusion

This study upholds a newly designed sensitive and selective bienzymatic biosensor for glucose detection with co-immobilization of GOx and HRP with polymerized multiporous nanofiber of SnO_2 onto glassy carbon electrode using chitosan. The morphological features of synthesized SnO_2 nanofiber and polymerized MPNFs of SnO_2 were scrutinized with the FESEM observation. Moreover, decontamination from impurities of the synthesized nanofiber is verified through EDX spectrum. The amperometric response of the fabricated biosensor possessed long-range linearity to the concentration of glucose. Furthermore, the fabricated biosensor sets out fast response and low detection limit with long-time stability and repeatability. Overall features of the biosensor direct the potentiality of it in sensitive detection of glucose in industry level and also the polymerized multiporous nanofiber of SnO_2 can be a promising nanomaterial for the future of biosensor.

References

[1] L. Zhu, R. Yang, J. Zhai, C. Tian, Bienzymatic glucose biosensor based on co-immobilization of peroxidase and glucose oxidase on a carbon nanotubes electrode, Biosensors and Bioelectronics 23(4) (2007) 528-535.

[2] Y. Sun, Y. Bai, W. Yang, C. Sun, Controlled multilayer films of sulfonate-capped gold nanoparticles/thionine used for the construction of a reagentless bienzymatic glucose biosensor, Electrochimica Acta 52(25) (2007) 7352-7361.

[3] M. Chen, C. Hou, D. Huo, M. Yang, H. Fa, An ultrasensitive electrochemical DNA biosensor based on a copper oxide nanowires/single-walled carbon nanotubes nanocomposite, Applied Surface Science 364 (2016) 703-709.

[4] B. Dalkıran, P.E. Erden, E. Kılıç, Amperometric biosensors based on carboxylated multiwalled carbon nanotubes-metal oxide nanoparticles-7, 7, 8, 8-tetracyanoquinodimethane composite for the determination of xanthine, Talanta 167 (2017) 286-295.

[5] J. Huang, G. Yue, J. Yang, S. Bai, Q. Hu, L. Wang, Design, synthesis and application of carboxylic multi-walled carbon nanotubes/tetrahexahedral platinum nanocrystals nanocomposites biosensor for simultaneous determination of guanine and adenine in DNA, Journal of Electroanalytical Chemistry (2017).

[6] Y.-Z. Zhang, H. Pang, Y. Sun, W.-Y. Lai, A. Wei, W. Huang, Porous tin oxide nanoplatelets as excellent-efficiency photoelectrodes and gas sensors, Int. J. Electrochem. Sci 8 (2013) 3371-3378.

[7] Q. Zhou, L. Yang, G. Wang, Y. Yang, Acetylcholinesterase biosensor based on SnO2 nanoparticles–carboxylic graphene–nafion modified electrode for detection of pesticides, Biosensors and Bioelectronics 49 (2013) 25-31.

[8] Q. Wali, A. Fakharuddin, I. Ahmed, M.H. Ab Rahim, J. Ismail, R. Jose, Multiporous nanofibers of SnO2 by electrospinning for high efficiency dye-sensitized solar cells, Journal of Materials Chemistry A 2(41) (2014) 17427-17434.

[9] N. Lavanya, S. Radhakrishnan, C. Sekar, Fabrication of hydrogen peroxide biosensor based on Ni doped SnO2 nanoparticles, Biosensors and Bioelectronics 36(1) (2012) 41-47.

[10] B. Cai, W. Mao, Z. Ye, J. Huang, Facile fabrication of all-solid-state SnO2/NiCo2O4 biosensor for self-powered glucose detection, Applied Physics A 122(9) (2016) 806.

[11] A.K.M. Kafi, Q. Wali, R. Jose, T.K. Biswas, M.M. Yusoff, A glassy carbon electrode modified with SnO2 nanofibers, polyaniline and hemoglobin for improved amperometric sensing of hydrogen peroxide, Microchimica Acta 184(11) (2017) 4443-4450.

[12] Q. Wali, A. Fakharuddin, I. Ahmed, M.H. Ab Rahim, J. Ismail, R. Jose, Multiporous nanofibers of SnO 2 by electrospinning for high efficiency dye-sensitized solar cells, Journal of Materials Chemistry A 2(41) (2014) 17427-17434.

[13] S. Alim, A.K.M. Kafi, R. Jose, M.M. Yusoff, J. Vejayan, Enhanced direct electron transfer of redox protein based on multiporous SnO2 nanofiber-carbon nanotube nanocomposite and its application in biosensing, International Journal of Biological Macromolecules 114,(2018) 1071-1076.

[14] E.I. Iwuoha, D. Saenz de Villaverde, N.P. Garcia, M.R. Smyth, J.M. Pingarron, Reactivities of organic phase biosensors. 2. The amperometric behaviour of horseradish peroxidase immobilised on a platinum electrode modified with an electrosynthetic polyaniline film, Biosensors and Bioelectronics 12(8) (1997) 749-761.

[15] Z. Liu, J. Wang, D. Xie, G. Chen, Polyaniline-Coated Fe3O4 Nanoparticle–Carbon-Nanotube Composite and its Application in Electrochemical Biosensing, Small 4(4) (2008) 462-466.

[16] Q. Xu, S.-X. Gu, L. Jin, Y.-e. Zhou, Z. Yang, W. Wang, X. Hu, Graphene/polyaniline/gold nanoparticles nanocomposite for the direct electron transfer of glucose oxidase and glucose biosensing, Sensors and Actuators B: Chemical 190 (2014) 562-569.

[17] X. Luo, A.J. Killard, A. Morrin, M.R. Smyth, Enhancement of a conducting polymer-based biosensor using carbon nanotube-doped polyaniline, Analytica Chimica Acta 575(1) (2006) 39-44.

[18] C. Dhand, M. Das, M. Datta, B. Malhotra, Recent advances in polyaniline based biosensors, Biosensors and Bioelectronics 26(6) (2011) 2811-2821.

[19] X. Feng, H. Cheng, Y. Pan, H. Zheng, Development of glucose biosensors based on nanostructured graphene-conducting polyaniline composite, Biosensors and Bioelectronics 70 (2015) 411-417.

[20] M. Guler, V. Turkoglu, A. Kivrak, A novel glucose oxidase biosensor based on poly([2,2′;5′,2″]-terthiophene-3′-carbaldehyde) modified electrode, International Journal of Biological Macromolecules 79 (2015) 262-268.

[21] Y. Shi, S.R. Crouch, Micro-scale determination of glucose by capillary flow injection with an immobilized enzyme reactor, Analytica Chimica Acta 381(2) (1999) 165-173.

[22] M. Chen, W.-P. Cai, Q.-Z. Zhu, X.-S. Wang, J.-G. Xu, Determination of glucose based on the effect of photons as a substitute for glucose oxidase, Analytica Chimica Acta 388(1) (1999) 11-17.

[23] K. Sugawara, T. Takano, H. Fukushi, S. Hoshi, K. Akatsuka, H. Kuramitz, S. Tanaka, Glucose sensing by a carbon-paste electrode containing chitin modified with glucose oxidase, Journal of Electroanalytical Chemistry 482(1) (2000) 81-86.

[24] A. Kafi, D.-Y. Lee, S.-H. Park, Y.-S. Kwon, DNA as a support for glucose oxidase immobilization at Prussian blue-modified glassy carbon electrode in biosensor preparation, Journal of nanoscience and nanotechnology 6(11) (2006) 3539-3542.

[25] P.A. Fiorito, C.M.A. Brett, S.I. Córdoba de Torresi, Polypyrrole/copper hexacyanoferrate hybrid as redox mediator for glucose biosensors, Talanta 69(2) (2006) 403-408.

[26] J.Z. Xu, J.J. Zhu, Q. Wu, Z. Hu, H.Y. Chen, An amperometric biosensor based on the coimmobilization of horseradish peroxidase and methylene blue on a carbon nanotubes modified electrode, Electroanalysis 15(3) (2003) 219-224.

[27] X. Wang, H. Gu, F. Yin, Y. Tu, A glucose biosensor based on Prussian blue/chitosan hybrid film, Biosensors and Bioelectronics 24(5) (2009) 1527-1530.

[28] J. Zhu, X. Liu, X. Wang, X. Huo, R. Yan, Preparation of polyaniline–TiO2 nanotube composite for the development of electrochemical biosensors, Sensors and Actuators B: Chemical 221 (2015) 450-457.

[29] S. Alim, P. Jaya Vejayan, K. AKM, Direct Electrochemistry of Catalase Immobilized at Polymerized-SnO2 Multiporous Modified Electrode for an Amperometric H2O2 Biosensor, Biomedical Journal of Scientific and Technical Research 3(4) (2018) 1-6.

[30] A. Kafi, M.J. Crossley, Synthesis of a conductive network of crosslinked carbon nanotube/hemoglobin on a thiol-modified Au Surface and its application to biosensing, Biosensors and Bioelectronics 42 (2013) 273-279.

[31] X. Ren, X. Meng, D. Chen, F. Tang, J. Jiao, Using silver nanoparticle to enhance current response of biosensor, Biosensors and Bioelectronics 21(3) (2005) 433-437.

[32] H.B. Dunford, Horseradish peroxidase: structure and kinetic properties, Peroxidase in chemistry and biology (1991) 1-23.

[33] S. Ko, Y. Takahashi, H. Fujita, T. Tatsuma, A. Sakoda, K. Komori, Peroxidase-modified cup-stacked carbon nanofiber networks for electrochemical biosensing with adjustable dynamic range, RSC Advances 2(4) (2012) 1444-1449.

[34] P. Benvenuto, A.K.M. Kafi, A. Chen, High performance glucose biosensor based on the immobilization of glucose oxidase onto modified titania nanotube arrays, Journal of Electroanalytical Chemistry 627(1) (2009) 76-81.

[35] P. Naderi Asrami, S.A. Mozaffari, M. Saber Tehrani, P. Aberoomand Azar, A novel impedimetric glucose biosensor based on immobilized glucose oxidase on a CuO-Chitosan nanobiocomposite modified FTO electrode, International Journal of Biological Macromolecules 118 (2018) 649-660.

[36] M. Baghayeri, H. Veisi, M. Ghanei-Motlagh, Amperometric glucose biosensor based on immobilization of glucose oxidase on a magnetic glassy carbon electrode modified with a novel magnetic nanocomposite, Sensors and Actuators B: Chemical 249 (2017) 321-330.

[37] T. Terse-Thakoor, K. Komori, P. Ramnani, I. Lee, A. Mulchandani, Electrochemically Functionalized Seamless Three-Dimensional Graphene-Carbon Nanotube Hybrid for Direct Electron Transfer of Glucose Oxidase and Bioelectrocatalysis, Langmuir 31(47) (2015) 13054-13061.

[38] R. Devasenathipathy, V. Mani, S.-M. Chen, S.-T. Huang, T.-T. Huang, C.-M. Lin, K.-Y. Hwa, T.-Y. Chen, B.-J. Chen, Glucose biosensor based on glucose oxidase immobilized at gold

nanoparticles decorated graphene-carbon nanotubes, Enzyme and Microbial Technology 78 (2015) 40-45.

[39] S. Palanisamy, C. Karuppiah, S.-M. Chen, Direct electrochemistry and electrocatalysis of glucose oxidase immobilized on reduced graphene oxide and silver nanoparticles nanocomposite modified electrode, Colloids and Surfaces B: Biointerfaces 114 (2014) 164-169.

[40] A. Kausaite-Minkstimiene, R. Simanaityte, A. Ramanaviciene, L. Glumbokaite, A. Ramanavicius, Reagent-less amperometric glucose biosensor based on a graphite rod electrode layer-by-layer modified with 1,10-phenanthroline-5,6-dione and glucose oxidase, Talanta 171 (2017) 204-212.

Table 1. Comparison of the performance of different glucose biosensor.

Electrode	LOD	Stability	References
GOx/Ag@MWCNT-IL-Fe_3O_4	3.8 μM	93% after 14 days	[36]
GOx/Graphene oxide-carbon nanotube hybrid	0.5 mM		[37]
GOx/Gold nanoparticles decorated graphene-carbon nanotubes	4.1 μM	94.37% after 60 days	[38]
GOx/Reduced graphene oxide and silver nanoparticles	0.16 mM	87.3 after 14 days	[39]
GOx/1,10-phenanthroline-5,6-dione (PD)	0.025 mM	23% after 16 days	[40]
GOx-HRP/PANI/SnO_2-NFs/Ch	1.8 μM	94% after 60 days	This work

Highlights

- A Novel platform for designing a glucose biosensor based on a polymerized-Multiporous SnO_2 Nanofibers/HRP/GOx electrode.

- For the first time, Polyaniline modified multiporous SnO_2 nanofiber has been applied for in developing glucose biosensors.

- The longer linear range, low LOD and quick response time in the sensing are really noteworthy.

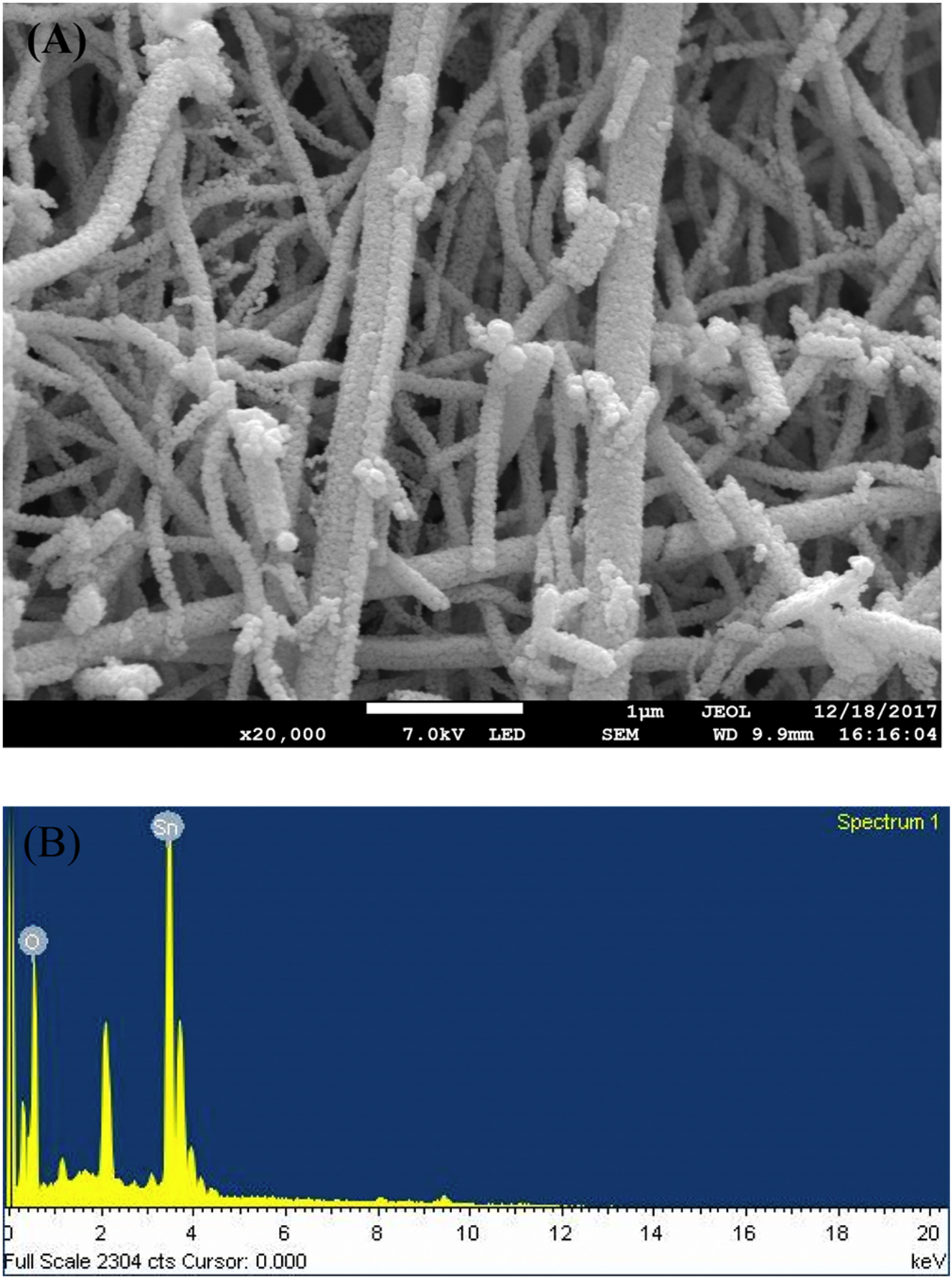
(A)
1µm JEOL 12/18/2017
x20,000 7.0kV LED SEM WD 9.9mm 16:16:04
(B)
Spectrum 1
Sn
O
0 2 4 6 8 10 12 14 16 18 20
Full Scale 2304 cts Cursor: 0.000
keV

Figure 1

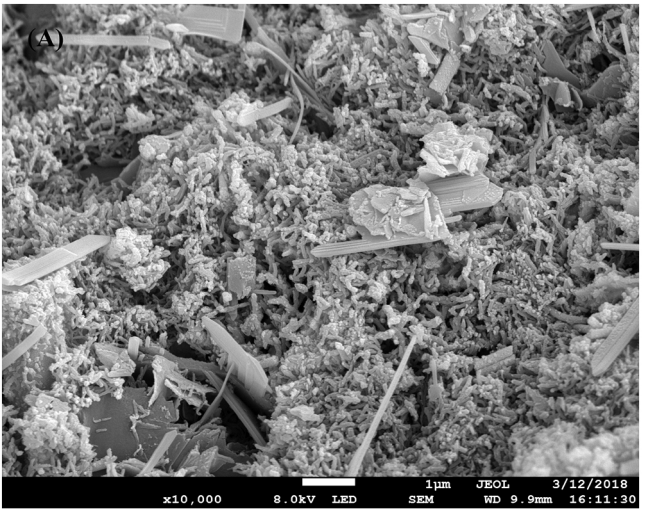
(A)
1µm JEOL 3/12/2018
x10,000 8.0kV LED SEM WD 9.9mm 16:11:30

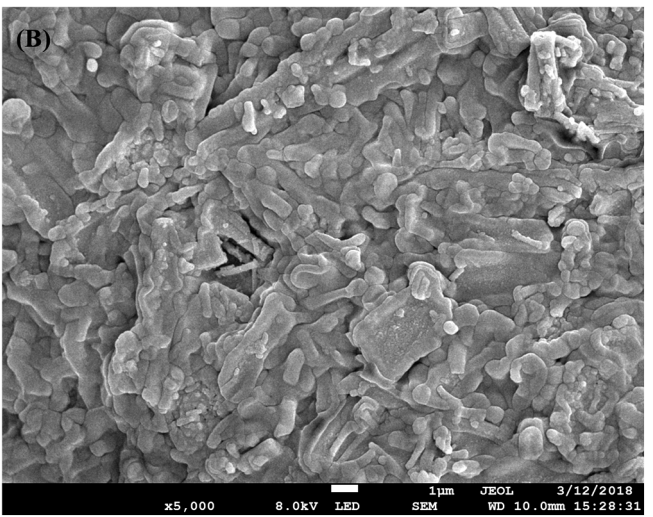
(B)
1µm JEOL 3/12/2018
x5,000 8.0kV LED SEM WD 10.0mm 15:28:31

Figure 2

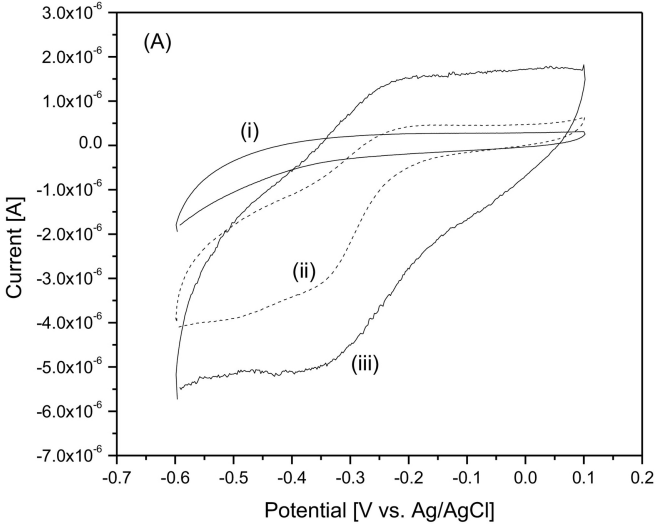
(A)
(i)
(ii)
(iii)
Current [A]
Potential [V vs. Ag/AgCl]
3.0x10-6
2.0x10-6
1.0x10-6
0.0
-1.0x10-6
-2.0x10-6
-3.0x10-6
-4.0x10-6
-5.0x10-6
-6.0x10-6
-7.0x10-6
-0.7
-0.6
-0.5
-0.4
-0.3
-0.2
-0.1
0.0
0.1
0.2

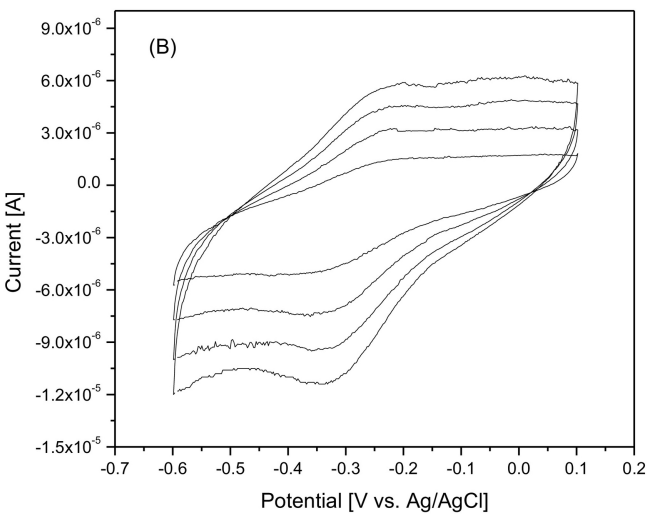
(B)
Current [A]
Potential [V vs. Ag/AgCl]
9.0x10-6
6.0x10-6
3.0x10-6
0.0
-3.0x10-6
-6.0x10-6
-9.0x10-6
-1.2x10-5
-1.5x10-5
-0.7
-0.6
-0.5
-0.4
-0.3
-0.2
-0.1
0.0
0.1
0.2

Figure 3

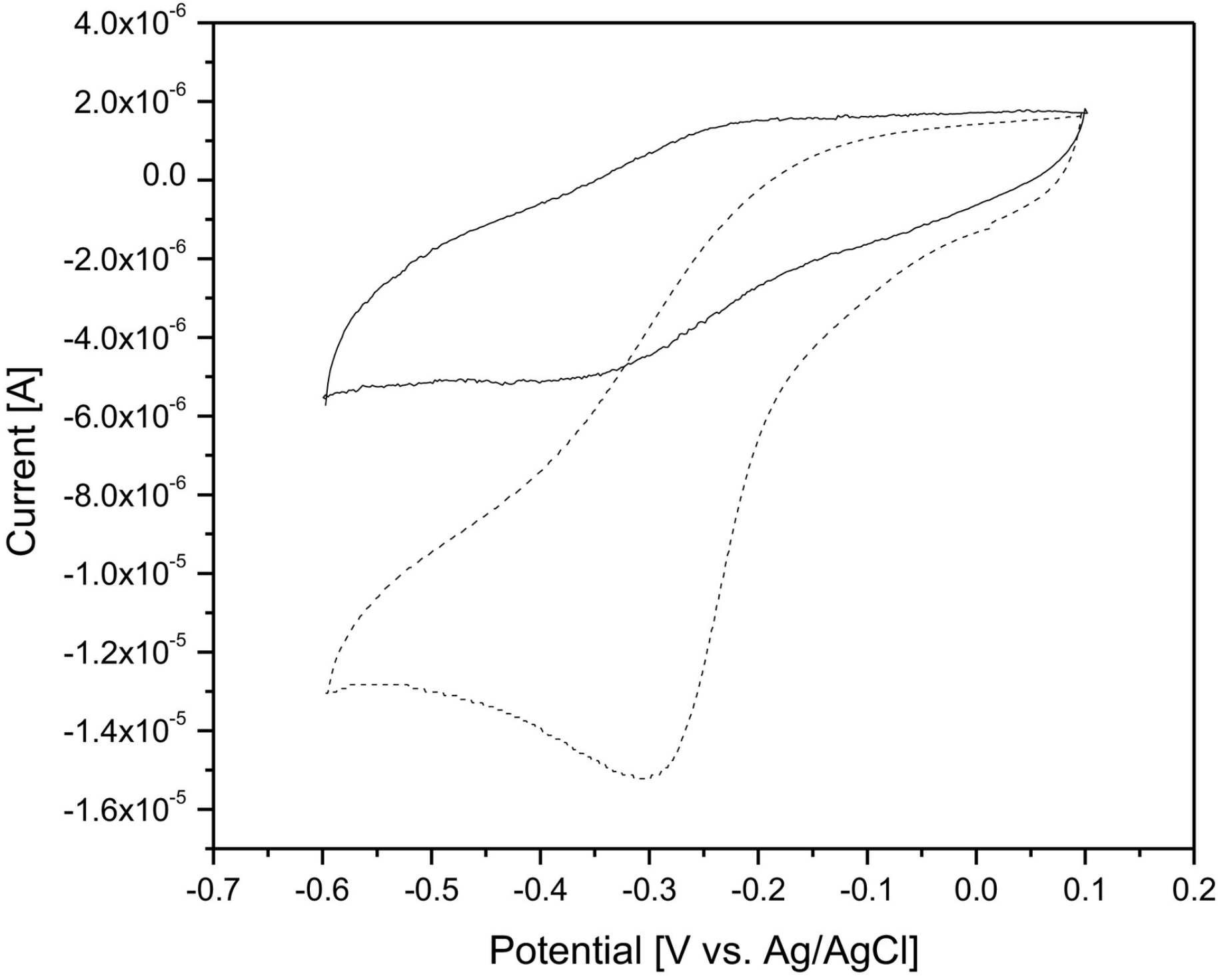
4.0x10-6
2.0x10-6
0.0
-2.0x10-6
-4.0x10-6
-6.0x10-6
-8.0x10-6
-1.0x10-5
-1.2x10-5
-1.4x10-5
-1.6x10-5
Current [A]
-0.7
-0.6
-0.5
-0.4
-0.3
-0.2
-0.1
0.0
0.1
0.2
Potential [V vs. Ag/AgCl]

Figure 4

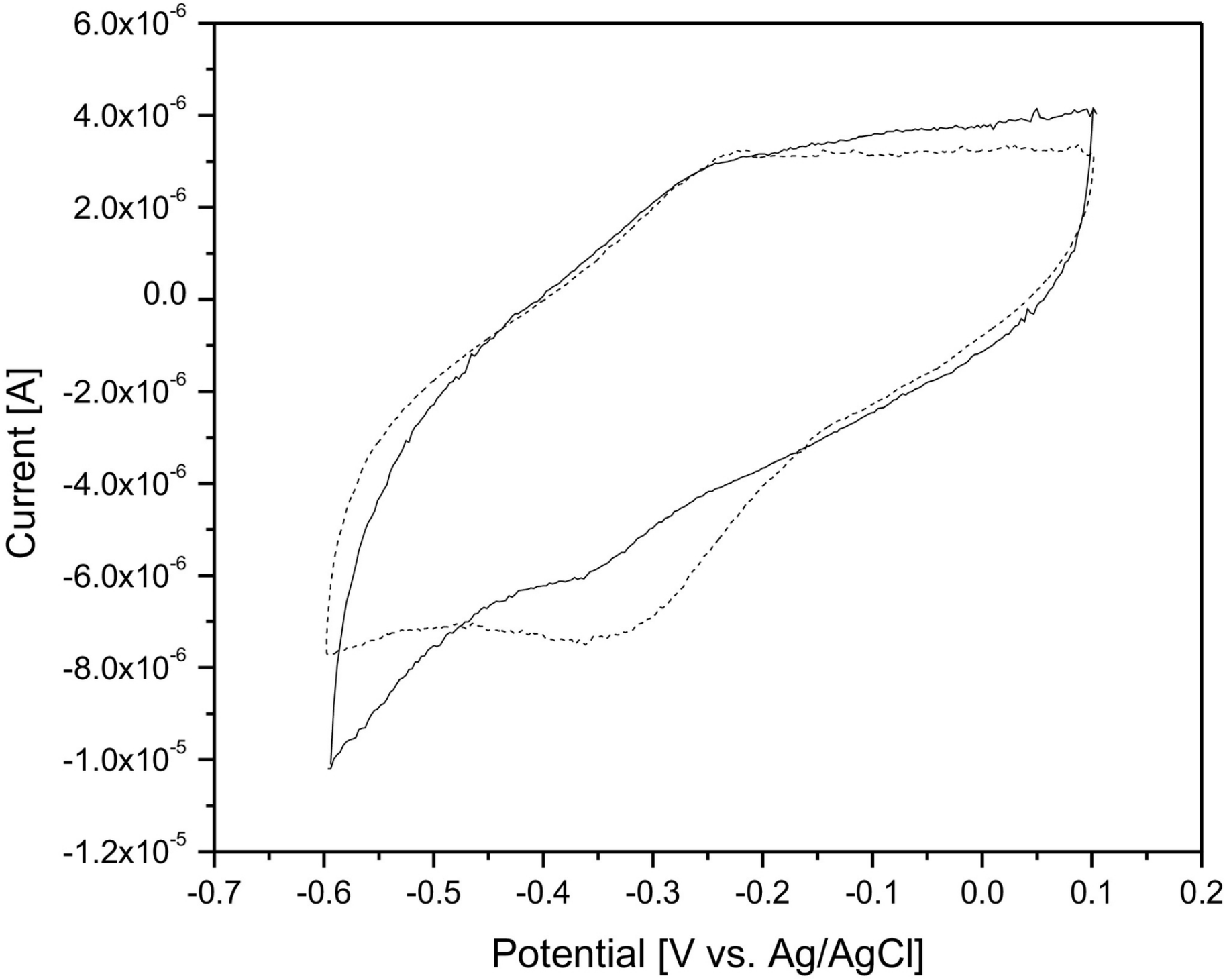
6.0x10-6
4.0x10-6
2.0x10-6
0.0
-2.0x10-6
-4.0x10-6
-6.0x10-6
-8.0x10-6
-1.0x10-5
-1.2x10-5
Current [A]
-0.7
-0.6
-0.5
-0.4
-0.3
-0.2
-0.1
0.0
0.1
0.2
Potential [V vs. Ag/AgCl]

Figure 5

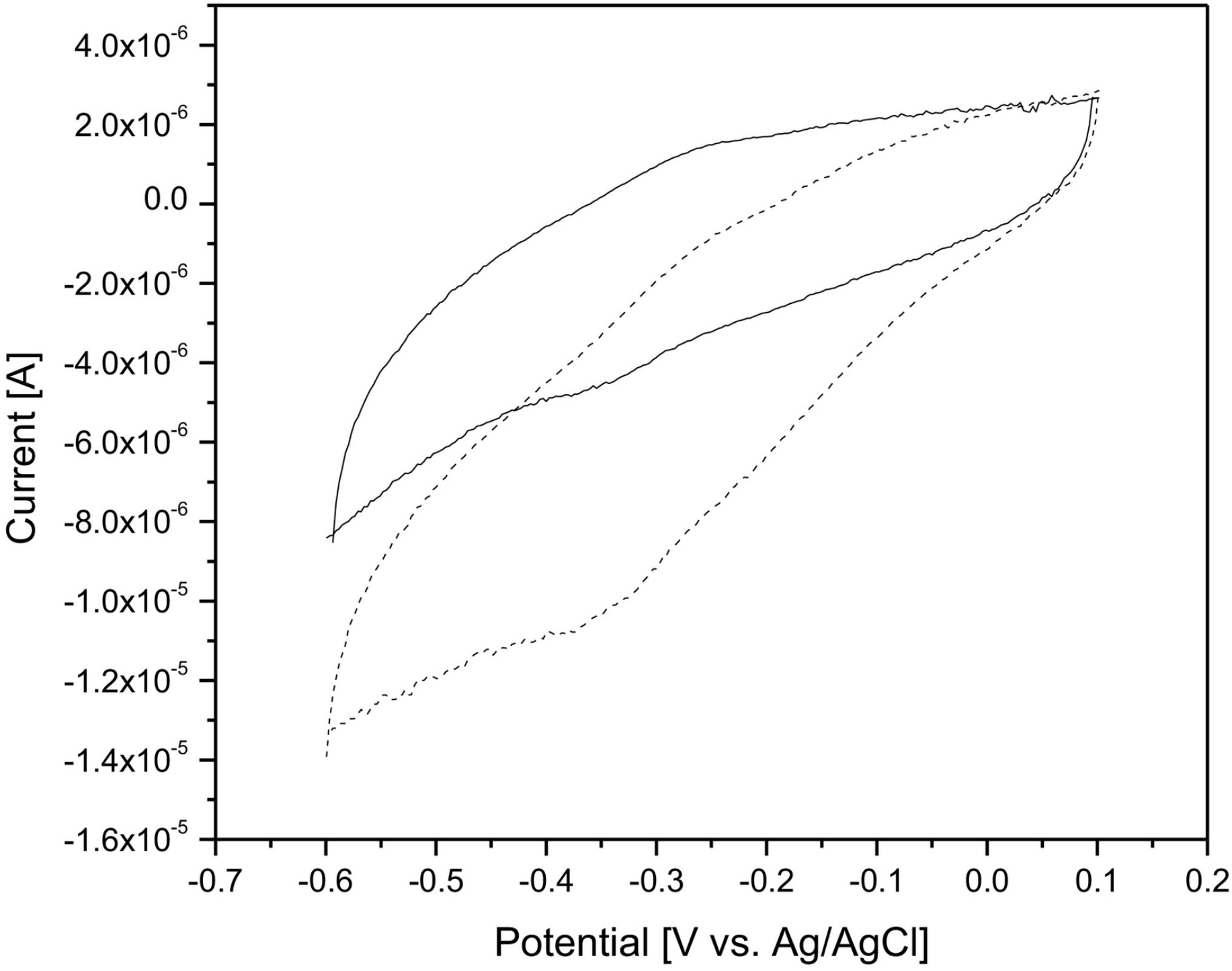
4.0x10-6
2.0x10-6
0.0
-2.0x10-6
-4.0x10-6
-6.0x10-6
-8.0x10-6
-1.0x10-5
-1.2x10-5
-1.4x10-5
-1.6x10-5
Current [A]
-0.7
-0.6
-0.5
-0.4
-0.3
-0.2
-0.1
0.0
0.1
0.2
Potential [V vs. Ag/AgCl]

Figure 6

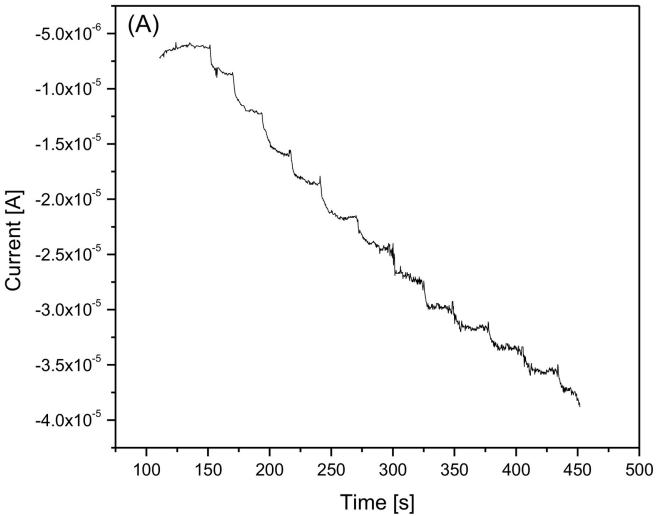
(A)
-5.0x10-6
-1.0x10-5
-1.5x10-5
-2.0x10-5
-2.5x10-5
-3.0x10-5
-3.5x10-5
-4.0x10-5
Current [A]
100
150
200
250
300
350
400
450
500
Time [s]

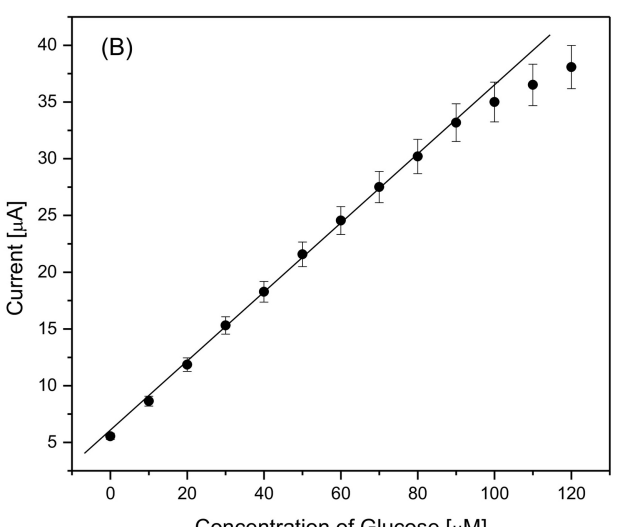
(B)
40
35
30
25
20
15
10
5
Current [μA]
0
20
40
60
80
100
120
Concentration of Glucose [μM]

Figure 7

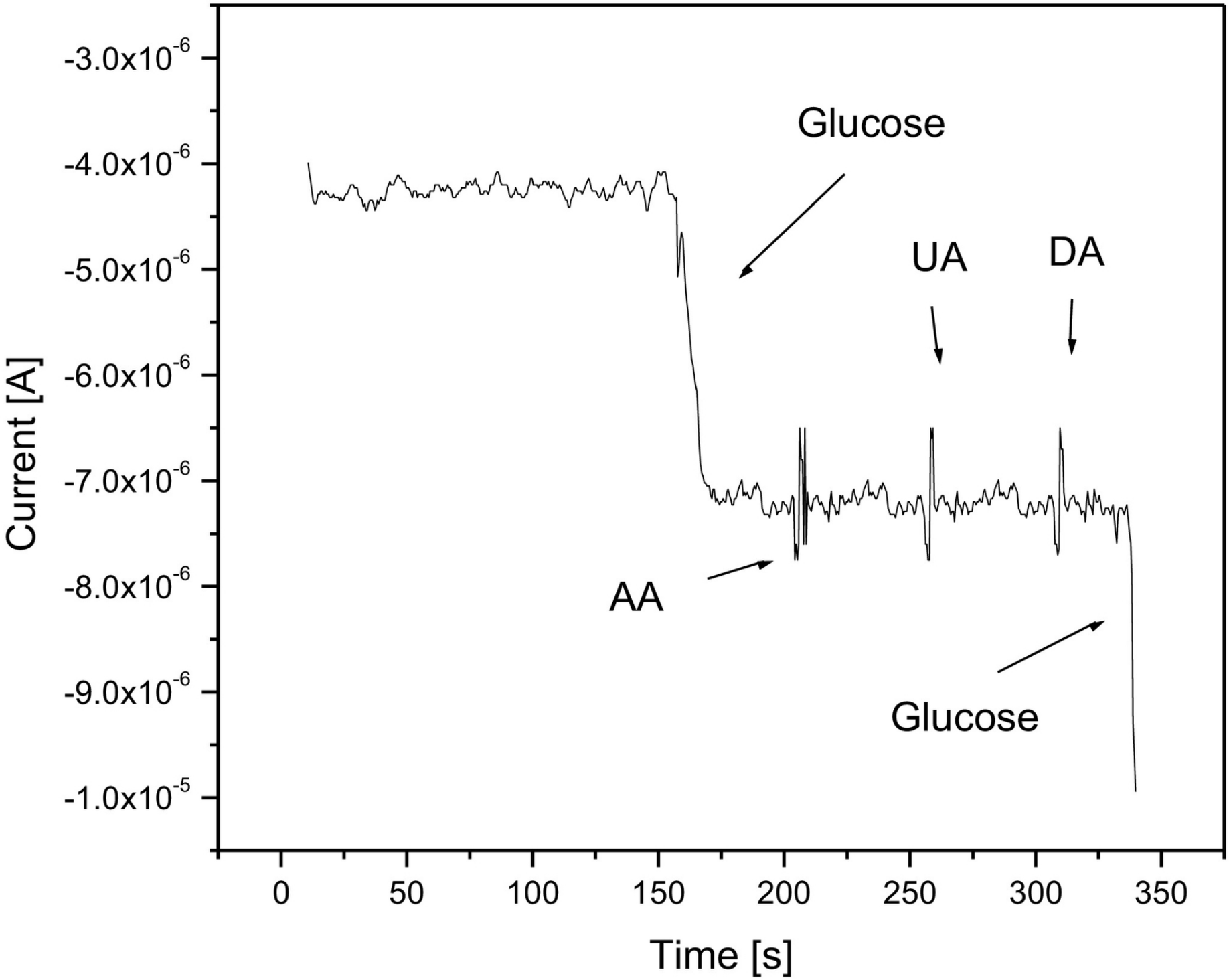
-3.0x10-6
-4.0x10-6
-5.0x10-6
-6.0x10-6
-7.0x10-6
-8.0x10-6
-9.0x10-6
-1.0x10-5
Current [A]
0
50
100
150
200
250
300
350
Time [s]
Glucose
UA
DA
AA
Glucose

Figure 8